

Template-Free Preparation of Bunches of Aligned Boehmite Nanowires

Jun Zhang, Siyi Wei, Jing Lin, Junjie Luo, Sujing Liu, Haisheng Song, Ellssfah Elawad, Xiaoxia Ding, Jianming Gao, Shouren Qi, and Chengcun Tang*

College of Physical Science and Technology, Central China Normal University, Wuhan 430079, China

Received: July 25, 2006; In Final Form: September 2, 2006

A simple method based on a hydrothermal process using alkali salts as mineralizers is proposed for the synthesis of aligned bunches of boehmite (γ -AlOOH) nanowires without a template's assistance. Most bunches of aligned boehmite nanowires are constructed by two separated shorter bundles with widths of 700 to \sim 800 nm and lengths of about 1 μ m. XRD patterns, FTIR spectra, and SEM and TEM images were used to characterize the products. The specific surface area and pore-size distribution of the obtained product as determined by gas-sorption measurements show that the boehmite bundles possess a high BET surface area and porosity properties. The importance of adding $\text{Na}_2\text{B}_4\text{O}_7$ salts for the formation of bundle morphologies has been discussed.

Introduction

Recently, one-dimensional (1-D) nanostructures (nanowires, nanotubes, and nanobelts) have been a focus of extensive research, due to their unique optical, electrical, and mechanical properties, which are different from those of the bulk materials.^{1–4} Generally speaking, 1-D nanomaterials can be fabricated by template-directed growth methods, such as by using carbon nanotubes,⁵ channels etched in porous materials, or scaffolds self-assembled from surfactants or block-copolymers,⁶ vapor–solid (VS),^{7,8} and vapor–liquid–solid (VLS) mechanisms.⁹ Owing to the great chemical flexibility and synthetic tunability in the solution-phase synthesis, the solution-based approaches provide a simple process toward such nanomaterials, using either multiple-source precursors or single-source precursors.¹⁰ Because of significant advantages, such as controllable particle size, low temperature, cost-effective and less-complicated techniques, hydrothermal processes have emerged as powerful tools for the fabrication of anisotropic nanomaterials.

Furthermore, for novel technologies based on nanoscale machines and devices, we not only need to prepare 1-D nanomaterials but also try to organize them into well-aligned patterns of nanocrystals since this may provide easier transport processes through nanostructured materials and have potential applications in light-emission/detection, field emission, biomedical devices, electrode materials in batteries, and so on.^{11–13} One of the most common techniques used to fabricate such nanostructures is the so-called template synthesis. For example, the porous alumina-based template technique has been used for the fabrication of metal and semiconductor nanowire arrays.^{14,15} On the other hand, the template-free synthesis of nanowire arrays, usually involving vapor-phase processes, has also been achieved. The ability to generate aligned and ordered nanocrystallites onto a substrate is typically reached by using masking/patterning techniques such as template or lithography.^{16,17} However, the introduction of templates into the synthetic routes makes the process troublesome and sometimes difficult to handle, and the vapor-phase process onto a substrate is still complicated and

low yielding. Therefore, developing rational and general strategies for the preparation of highly ordered 1-D nanomaterials is a very significant orientation in the exploitation of these building units and is of great importance for commercial purposes.

Alumina is one of the most important oxides and has been studied intensively over a long period of time because of its potential for broad applications in adsorbents, catalysts, and catalyst supports.¹⁸ The synthesis of nanostructured alumina, especially 1-D nanostructures, has received considerable interest due to their novel properties, such as high elastic modulus, thermal and chemical stability, and optical characteristics.^{19,20} The γ -alumina can be obtained through the dehydration of the boehmite form of γ -AlOOH at temperatures in the range of 400 to \sim 700 °C. During heating, the boehmite nanostructures undergo an isomorphous transformation to nanocrystalline γ -alumina, and the products can retain the morphology of the parent boehmite nanostructures.^{21,22} Therefore, various morphologies of boehmite nanostructures have been synthesized, such as nanoparticles,²³ nanofibers,^{24,25} nanobelts,²⁶ nanotubes,^{27,28} and flower-like 3-D nanoarchitectures.²⁹

However, to our knowledge, there are less reports about well-aligned arrays of boehmite or alumina nanowires, in which the anodic alumina membrane (AAM) with ordered nanochannels is adopted.^{30,31} Herein, we report a template-free hydrothermal route to fabricate aligned bunches of boehmite nanowires using alkali salts as mineralizers. Comparative experiments show that the addition of salts is a key factor. We speculated that the mineralizers may favor the growth of 1-D nanowires and decorate their surfaces for the formation of bundles. In addition, the specific surface area and pore-size distribution of the obtained products were also investigated.

Experimental Procedures

In a typical procedure, analytical pure $\text{AlCl}_3 \cdot 6\text{H}_2\text{O}$ (0.724 g, 0.003 mol) was dissolved into 30 mL of distilled water at room temperature in a beaker and magnetically stirred to form a homogeneous solution. Then, 15 mL of $\text{Na}_2\text{B}_4\text{O}_7 \cdot 10\text{H}_2\text{O}$ (0.1 M) aqueous solution was added dropwise to the previously solution. Magnetic stirring (2000 rpm) was maintained throughout the entire process and lasted for 10 min. The resulting clear

* To whom correspondence should be addressed. Fax: + 86-27-67861185. Tel: +86-27-67861185. E-mail: cctang@phy.ccnu.edu.cn.

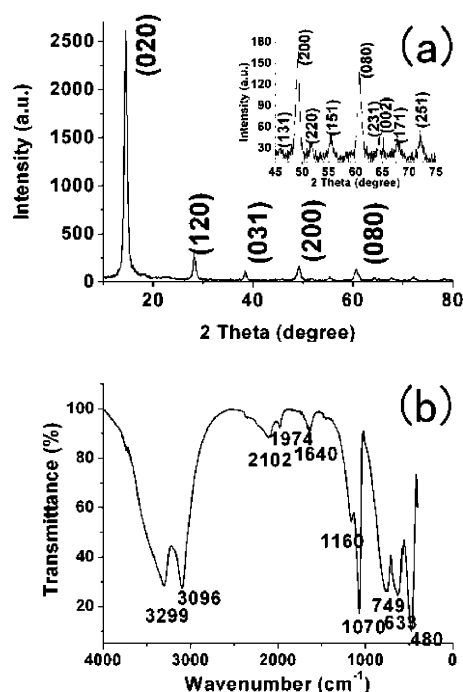


Figure 1. (a) Typical XRD pattern, the enlarged portion (inset) and (b) infrared spectrum of the products.

and colorless solution was transferred into a Teflon-lined stainless autoclave up to 85% of the total volume. The autoclave was sealed and maintained at 200 °C for 24 h and then allowed to cool naturally to room temperature. A white precipitate was obtained. The product was washed and filtered several times with distilled water and then dried in a vacuum at 60 °C for 12 h.

The crystal structure and phase purity of the product were examined by means of X-ray diffraction (XRD, D/max-rB, Cu K α radiation) analysis. The overview of the sample morphology was checked by scanning electron microscopy (SEM, JSM-6700F, JEOL), equipped with the system of energy-dispersive spectroscopy (EDS) analysis. The sample powder was ultrasonically dispersed in acetone and dropped onto a carbon coated copper grid for transmission electron microscopy (TEM, JEM-2010F, JEOL) measurement. Fourier transform infrared (FTIR) spectroscopy (Nicolet 170-SX) was utilized to characterize the product. The nitrogen adsorption and desorption isotherms at 77 K were measured using a Micrometrics ASAP 2020 V3.00 H system after the sample was degassed in a vacuum at 120 °C for 400 min.

Results and Discussion

XRD analysis was used to determine the structure and phase of the sample. Figure 1a shows the X-ray diffraction pattern of the as-prepared product. All detectable peaks in this pattern can be assigned by their peak position to the orthorhombic γ -AlOOH, which can be identified by the enlarged portion shown in the inset of Figure 1a. As compared with the standard diffraction peaks formed (JCPDS Card 21-1307), no other peak was observed belonging to the impurities, such as Na₂B₄O₇ or NaCl, indicating the high purity of the as-obtained sample. More specifically, it can be observed that the intensity of the peak with 2θ values of 14.50 corresponding to the (020) crystal plane is extraordinarily strong as compared to other peaks. This phenomenon may be caused by preferential growth of the nanowire and aligned bundle structure. Moreover, the obtained sample was further examined by FTIR analysis shown in Figure

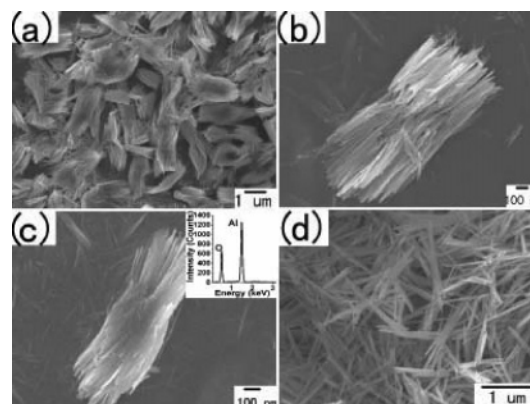


Figure 2. (a) Low-magnification SEM image of the γ -AlOOH bundles; (b) high-magnification SEM images of two separated bundles connected loosely and (c) closely and EDS pattern (inset) of the products; and (d) representative SEM image of irregular nanowires obtained when the Na₂B₄O₇ salts were replaced by a NaOH solution while keeping the value of the pH same.

1b. It is clear that the boehmite prepared by the simple hydrothermal conditions showed absorption bands at 3299, 3096, 2102, 1974, 1640, 1160, 1070, 749, 633, and 480 cm⁻¹, which agree precisely with those reported in the literature.³² In detail, the intensive bands at 3299 and 3096 cm⁻¹ can be assigned to the ν_{as} (Al)O-H and ν_s (Al)O-H stretching vibrations. The two weak bands at 2102 and 1974 cm⁻¹ can be assigned to combination bands. The intense band at 1070 cm⁻¹ and the shoulder at 1160 cm⁻¹ are ascribed to the δ_s Al-O-H and δ_{as} Al-O-H bending vibrations in the boehmite lattice. The three strong bands at 749, 633, and 749 cm⁻¹ can be assigned to the vibration mode of AlO₆. In addition, the shoulder at 1640 cm⁻¹ can be assigned to the bending mode of adsorbed water. Consequently, FTIR analysis also confirms that the as-obtained product is pure-phase γ -AlOOH.

The morphology of the as-obtained product was examined by SEM. Figure 2a shows the whole image of the product. Interestingly, the particles of the sample are highly dispersed, and each one is bundle-like and composed of many side-by-side nanowires. Each bunch has average widths of 700 to ~800 nm and lengths of about 1 to ~2 μ m. After closer observation, we found that most bunches of aligned boehmite nanowires are constructed by two separated shorter ones, which can be observed clearly from the high-magnification images shown in Figure 2b,c. It can be seen that the two separated bundles connect together head-to-head and arrange in a line. Two connection models can be observed. Figure 2b shows that the two bundles connect loosely with vacancies existing in the middle part located between each two bundle branches. Different from Figure 2 panel b, panel c shows two separated bundles joined together, in which no vacancy can be observed in the joint part and whose width is obviously larger than that of the two tips. EDS was conducted for chemical composition of the bundle structures, which revealed the presence of both aluminum and oxygen shown in the inset in Figure 2c. Quantitative results show that the value of the atomic ratio for O/Al is approximately 1.9, which is close to the ideal value of 2 considering the instrumental error.

The structure characterization of the γ -AlOOH nanowire bundles is investigated in detail by SAED and TEM microscopy. Figure 3a is a TEM image of two joined bundle structures, which were dispersed in absolute ethanol under ultrasonic vibration, indicating that the nanowires are closely packed together in this bunch. However, not all of the nanowires could arrange in a preferred orientation to form the bundles because we could

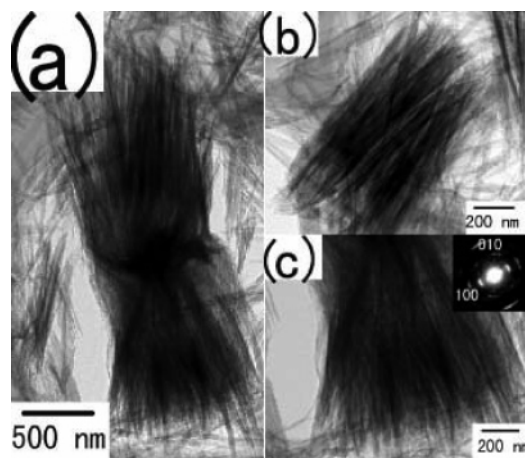


Figure 3. (a) TEM images of two joint bundles; (b) single bundle; (c) end-section of a bundle of the products; and (inset) the SAED result of the products.

observe some dispersed nanowires around the bundle. This phenomenon may be caused by the ultrasonic vibration and some of the nanowires separated from the surface of the bundles. On the side, we also observed a single bundle without connecting it with the other bundle as shown in Figure 3b. The end-section of the bunch shown in Figure 3c displays that these nanowires with an average diameter of about 20 nm are arrayed in an ordered fashion and are closely packed together. A typical SAED recorded with the electron beam perpendicular to the axis of the boehmite nanowire bundle is shown in the inset of Figure 3c, indicating the single-crystal nature of the sample. The SAED pattern can be indexed as an orthorhombic crystal recorded along the [001] zone axis. The pattern clearly indicates the orientation alignment among all of the nanowires in the bundle along [010], which shows that the nanowires are aligned not only in length but also in crystallographic orientation. In addition, the SAED pattern is characterized by the symmetrical stripes rather than polycrystalline circles or single-crystal spots, implying the presence of some ordered arrangement of crystallites in the bundle, which is in good agreement with the SEM and TEM observations.

In the experiment, the morphology and size of the AIOOH was found to depend strongly on the effects of the alkali salts $\text{Na}_2\text{B}_4\text{O}_7$. When the salts were absent, no white precipitate was obtained. Irregular nanowires were observed when the $\text{Na}_2\text{B}_4\text{O}_7$ salts were replaced by a NaOH solution, keeping the value of pH the same (Figure 2d). Thus, the presence of the salts is one of the important factors influencing the crystallization process and the growth of the boehmite nanowire bundles.

One effect of the $\text{Na}_2\text{B}_4\text{O}_7$ salts is to increase the chemical potential of the solution, and higher chemical potential conditions would be advantageous for 1-D nanostructure growth.³³ The chemical potential is mainly determined by the pH value and solute concentrations of the solutions in the reaction system.³⁴ At the very beginning, the addition of the $\text{Na}_2\text{B}_4\text{O}_7 \cdot 10\text{H}_2\text{O}$ aqueous solution to the $\text{AlCl}_3 \cdot 6\text{H}_2\text{O}$ solution led to the formation of the amorphous colloid $\text{Al}(\text{OH})_3$. When the reaction was carried out at 200 °C, AIOOH was obtained from the early formed $\text{Al}(\text{OH})_3$ colloids. According to the suggestion of Pierre,³⁵ oxygen ions are arranged in a distorted octahedral configuration around aluminum in the boehmite (AIOOH) lattice and are organized in a parallel layer linked by hydrogen bonds. Because of the weak hydrogen bonds and the surface OH^- bond-induced interaction between the solvent molecules, the layer structure of AIOOH tends to curl at an elevated temperature

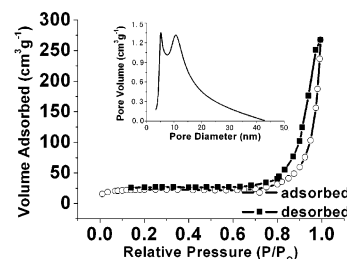


Figure 4. N_2 absorption and desorption isotherms and pore-size distributions (insets) for the γ -AIOOH bundles.

and pressure, leading to the formation of AIOOH 1-D nanowires via the rolling mechanism. This is a general process for the formation of nanowires through the folding of the lamella.³⁶ So, the addition of the $\text{Na}_2\text{B}_4\text{O}_7$ salts can provide a favorable environment for the growth of nanowires in our system.

In addition, the $\text{Na}_2\text{B}_4\text{O}_7$ salts should be responsible for the formation of boehmite nanowire bundles. The electric force via the addition of the $\text{Na}_2\text{B}_4\text{O}_7$ salts has been utilized in the bundle system.³⁷ As known, the Stern model is frequently used to describe the electric double layer at the interface between an oxide surface and water.³⁸ The main point in this research is that each particle in an aqueous suspension is surrounded by an electrostatic double layer (Stern layer). The thickness of the diffuse part in the double layer is inversely proportional to the square root of the ionic strength of the bulk solution. A higher ionic strength will increase the surface charge density by screening the electrostatic repulsion at the interface. Therefore, an increase in the ionic strength is manifested in a compression of the diffuse part of the double layer with a concomitant decrease in the repulsion between particles and a lowering of the interfacial tension of the system. The ionic strength is proportional to the concentrations of the individual ions and the square of their charges. So, the addition of the $\text{Na}_2\text{B}_4\text{O}_7$ salt solution in the reaction system could increase the ionic strength evidently, which reversely decreases the repulsion between nanowires and favors the formation of bundles. On the other side, specific adsorption of protons such as the $\text{B}_4\text{O}_7^{2-}$ ions in the Stern layer would dramatically decrease the surface charge and potential, which will decrease the internanowire repulsion. Hence, $\text{Na}_2\text{B}_4\text{O}_7$ salts play a key role in the formation of boehmite nanowire bundles in the adopted reaction system. However, the formation mechanism of bundle nanoarchitectures, especially the formation of two separated bundles connected in length, has not been fully understood. Determining the exact nature of the growth mechanism will require further theoretical and experimental works.

To investigate the specific surface area and porous nature of the boehmite nanowire bundles, Brunauer–Emmett–Teller (BET) gas-sorption measurements were carried out. The recorded nitrogen adsorption/desorption isotherms for the bundles showed significant hysteresis at relative pressures P/P_0 above 0.60 (Figure 4). The hysteresis loop can be categorized as type IV. The BET specific surface area of the sample is found to be as much as about $150.6 \text{ m}^2 \text{ g}^{-1}$ and is calculated from N_2 isotherms at 77 K. Music et al. have reported that the specific area decreased considerably with the increase of the boehmite crystallinity, and the best area reported so far for the crystallized sample is $91 \text{ m}^2 \text{ g}^{-1}$.³⁹ Therefore, the AIOOH bundles obtained here have an extremely high BET area. Barrett–Joyner–Halenda (BJH) calculations for the pore-size distribution, derived from desorption data, reveal a narrow distribution with double apexes centered at 5 to ~ 6 nm and 13 to ~ 14 nm, respectively (Figure 4, inset). The smaller pores presumably arise from the

spaces within a nanowire. The larger pores are possibly attributed to the internanowire spaces. The results display that the obtained boehmite bundles have excellent porous properties.

Conclusion

In summary, we have demonstrated a facile hydrothermal method to synthesize orthorhombic γ -AlOOH bundles with the assistance of $\text{Na}_2\text{B}_4\text{O}_7$ salts as mineralizers in the absence of any templates or matrixes. The addition of $\text{Na}_2\text{B}_4\text{O}_7$ salts was of great importance in the bundle formation process and played crucial roles, such as an increase in the chemical potential of the solution, a decrease in the internanowire repulsion by increasing the ionic strength, and offering the anion adsorption on the surface of nanowires. Although the formation mechanism of the nanowire bundles has not yet been fully understood, this easily conducted route may be extended to synthesize other metal oxide and hydroxide nanowire bundles with the assistance of alkali salts. Taking into account the single-crystal characteristics, high BET surface area, and excellent porous properties, γ -AlOOH bundles developed in the present work are promising candidates for technical applications in the areas of catalysts, sorbents, ceramics, and optical nanodevices.

Acknowledgment. This work was supported by the Fok Ying Tong Education Foundation (Grant 91050) and the NNSF of China (Grant 50202007).

References and Notes

- (1) Wong, E. W.; Sheehan, P. E.; Lieber, C. M. *Science* **1997**, 277, 1991.
- (2) Kong, J.; Soh, H.; Cassell, A. M.; Quate, C. F.; Dai, H. *Nature (London)* **1998**, 385, 878.
- (3) Xia, Y. N.; Yang, P. D.; Sun, Y. G.; Wu, Y. Y.; Mayers, B.; Gates, B.; Yin, Y. D.; Kim, F.; Yan, H. Q. *Adv. Mater.* **2003**, 15, 353.
- (4) Huang, Y.; Duan, X. F.; Lieber, C. M. *Small* **2005**, 1, 142.
- (5) Han, W. Q.; Fan, S. S.; Li, Q. Q.; Hu, Y. D. *Science* **1997**, 277, 1287.
- (6) Tsang, S. C.; Chen, Y. K.; Harris, P. J. F.; Green, M. L. H. *Nature (London)* **1994**, 372, 159.
- (7) Lao, J. Y.; Huang, J. Y.; Wang, D. Z.; Ren, Z. F. *Nano Lett.* **2003**, 3, 235.
- (8) Fang, X. S.; Zhang, L. D. *J. Mater. Sci. Technol.* **2006**, 22, 1.
- (9) Morales, A. M.; Lieber, C. M. *Science* **1998**, 279, 208.
- (10) Tang, C. C.; Bando, Y.; Golberg, D.; Ma, R. Z. *Angew. Chem., Int. Ed.* **2005**, 44, 576.
- (11) Huang, M. H.; Mao, S.; Feick, H.; Yan, H.; Wu, Y.; Weber, E.; Russo, R.; Yang, P. *Science* **2001**, 292, 1987.
- (12) Hatzor, A.; Weiss, P. S. *Science* **2001**, 291, 1019.
- (13) Wu, Y. H. B.; Yang, J.; Han, G. C.; Zong, B. Y.; Ni, H. Q.; Luo, P. T.; Chong, C.; Low, T. S.; Shen, Z. X. *Adv. Funct. Mater.* **2002**, 12, 489.
- (14) Cao, H. Q.; Xu, Z.; Sang, H.; Sheng, D.; Tie, C. Y. *Adv. Mater.* **2001**, 13, 121.
- (15) Cao, H. Q.; Xu, Y.; Hong, J. M.; Liu, H. B.; Yin, C.; Li, B. L.; Tie, Z. Y.; Xu, Z. *Adv. Mater.* **2001**, 13, 1393.
- (16) Ren, Z. F.; Huang, Z. P.; Xu, J. W.; Wang, J. H. *Science* **1998**, 282, 1105.
- (17) Wang, X. D.; Summers, C. J.; Wang, Z. L. *Nano Lett.* **2004**, 4, 423.
- (18) Raybaud, P.; Digne, M.; Iftimie, R.; Wellens, W.; Euzen, P.; Toulboat, H. *J. Catal.* **2001**, 201, 236.
- (19) Das, G. *Ceram. Eng. Sci. Proc.* **1995**, 16, 977.
- (20) Fang, X. S.; Ye, C. H.; Zhang, L. D.; Xie, T. *Adv. Mater.* **2005**, 17, 1661.
- (21) Lee, H. C.; Kim, H. J.; Chung, S. H.; Lee, K. H.; Lee, H. C.; Lee, J. S. *J. Am. Chem. Soc.* **2003**, 125, 2882.
- (22) Zhang, M.; Zhang, R.; Xi, G. C.; Liu, Y.; Qian, Y. T. *J. Nanosci. Nanotechnol.* **2006**, 6, 1437.
- (23) Naskar, M. K.; Chatterjee, M. *J. Am. Ceram. Soc.* **2005**, 88, 3322.
- (24) Kuiry, S. C.; Megen, E.; Patil, S. D.; Deshpande, S. A.; Seal, S. J. *Phys. Chem. B* **2005**, 109, 3686.
- (25) Tang, B.; Ge, J. C.; Zhou, L. H.; Wang, G. L.; Niu, J. Y.; Shi, Z. Q.; Dong, Y. B. *Eur. J. Inorg. Chem.* **2005**, 21, 4366.
- (26) Gao, P.; Xie, Y.; Chen, Y.; Ye, L. N.; Guo, Q. X. *J. Cryst. Growth* **2005**, 285, 555.
- (27) Kuang, D. B.; Fang, Y. P.; Liu, H. Q.; Frommen, C.; Fenske, D. *J. Mater. Chem.* **2003**, 13, 660.
- (28) Hou, H. W.; Xie, Y.; Yang, Q.; Guo, Q. X.; Tan, C. R. *Nanotechnology* **2005**, 16, 741.
- (29) Zhang, J.; Liu, S. J.; Lin, J.; Song, H. S.; Luo, J. J.; Elssaf, E. M.; Ammar, E.; Huang, Y.; Ding, X. X.; Qi, S. R.; Tang, C. J. *Phys. Chem. B* **2006**, 110, 14249.
- (30) Yuan, Z. H.; Huang, H.; Fan, S. S. *Adv. Mater.* **2002**, 14, 303.
- (31) Kim, J.; Choi, Y. C.; Chang, K. S.; Bu, S. D. *Nanotechnology* **2006**, 17, 355.
- (32) Kiss, A. B.; Keresztury, G.; Fakas, L. *Spectrochim. Acta, Part A* **1980**, 36, 653.
- (33) Wang, X.; Li, Y. D. *Angew. Chem., Int. Ed.* **2002**, 41, 4790.
- (34) Peng, Z. A.; Peng, X. G. *J. Am. Chem. Soc.* **2001**, 123, 1389.
- (35) Pierre, A. C.; Uhlmann, D. R. *J. Non-Cryst. Solids* **1986**, 82, 271.
- (36) Li, Y. D.; Li, X. L.; Deng, Z. X. *Angew. Chem., Int. Ed.* **2002**, 41, 333.
- (37) Gracias, D. H.; Tien, J.; Breen, T. L.; Hsu, C.; Whitesides, G. M. *Science* **2000**, 289, 1170.
- (38) Hiemenz, P. C. *Principles of Colloid and Surface Chemistry*; Marcel Dekker: New York, 1977; Chs. 1, 9, and 10.
- (39) Music, S.; Dragcevic, O.; Popovic, S. *Mater. Lett.* **1999**, 40, 26.